

## Electronic density response to molecular geometric changes from explicit electronic susceptibility calculations

Arvid Conrad Ihrig, Arne Scherrer, and Daniel Sebastiani

Citation: *The Journal of Chemical Physics* **139**, 094102 (2013); doi: 10.1063/1.4819070

View online: <http://dx.doi.org/10.1063/1.4819070>

View Table of Contents: <http://scitation.aip.org/content/aip/journal/jcp/139/9?ver=pdfcov>

Published by the [AIP Publishing](#)

---



## Re-register for Table of Content Alerts

Create a profile.



Sign up today!



# Electronic density response to molecular geometric changes from explicit electronic susceptibility calculations

Arvid Conrad Ihrig,<sup>1</sup> Arne Scherrer,<sup>1</sup> and Daniel Sebastiani<sup>2,a)</sup>

<sup>1</sup>*Dahlem Center for Complex Quantum Systems, Physics Department, Freie Universität Berlin, Arnimallee 14, 14195 Berlin, Germany*

<sup>2</sup>*Institute of Chemistry, Martin Luther University Halle-Wittenberg, Von-Danckelmann-Platz 4, 06120 Halle (Saale), Germany*

(Received 22 May 2013; accepted 8 August 2013; published online 3 September 2013)

We present a first principles approach to compute the response of the molecular electronic charge distribution to a geometric distortion. The scheme is based on an explicit representation of the linear electronic susceptibility. The linear electronic susceptibility is a tensor quantity which directly links the first-order electronic response density to the perturbation potential, without requiring self-consistency. We first show that the electronic susceptibility is almost invariant to small changes in the molecular geometry. We then compute the dipole moments from the response density induced by the geometrical changes. We verify the accuracy by comparing the results to the corresponding values obtained from the self-consistent calculations of the ground-state densities in both geometries.

© 2013 AIP Publishing LLC. [<http://dx.doi.org/10.1063/1.4819070>]

## I. INTRODUCTION

The equilibrium state of a physical system is of fundamental importance for understanding its structural properties. However, especially spectroscopic experiments often rely on excitations of the system of interest.<sup>1–5</sup> It is therefore necessary to include these excitations in the molecular simulation to link experiment and theory and gain a deeper understanding of the spectroscopic processes.<sup>6–12</sup> Since the perturbation causing the excitation is usually small compared to the Hamiltonian of the unperturbed ground-state, it is convenient to use perturbation theory. Within this framework, a multitude of external perturbations can be considered, such as electric and magnetic fields or the excitation of vibrational modes.<sup>13–22</sup> The latter, or phonons in the context of solids, are derivatives of the total energy with respect to all nuclear coordinates, which results in a set of  $3N$  perturbation calculations for a system with  $N$  atoms. Especially for small wavevectors  $q$ , which stretch across several unit cells, the number of required calculations grows quickly.<sup>15</sup> In view of this scaling, it is highly desirable to reduce the effort necessary for each perturbation calculation. An alternative to the most common scheme, a fully self-consistent perturbation calculation, is based on the linear electronic susceptibility, a tensor quantity which links the perturbation potential directly to the electronic response density.<sup>23–26</sup> Once computed for the system of interest, it therefore allows to perform perturbation calculations as simple matrix-vector products. In a first proof-of-principle article,<sup>26</sup> we have illustrated the algorithm and its potential for modelling supramolecular interactions at the level of density functional theory (DFT).<sup>27,28</sup>

Correctly predicting the response of the electronic state due to geometrical distortions is the key require-

ment for applying any perturbation theory to phonon calculations.<sup>4,12,29–31</sup> In this paper, we show that the linear electronic susceptibility is almost invariant to geometrical changes and well suited to predict the electronic response density by computing the dipole moments induced by the geometrical distortions.

Density functional perturbation theory is commonly expressed in terms of a linear system of equations for the perturbed orbital states:

$$(H_0 - \epsilon_i)\psi_i^1 = -H_1\psi_i^0, \quad (1)$$

where  $H_0$  is the unperturbed Hamiltonian operator,  $\epsilon_i$  the Kohn-Sham energy value for the unperturbed orbital  $\psi_i^0$ , and  $\psi_i^1$  is the perturbation correction due to the perturbation Hamiltonian  $H_1$ . The explicit dependence of the DFT Hamiltonian on the electronic density leads to an additional term on the right-hand side of this equation, which requires an iterative self-consistent approach for the numerical solution of  $\psi_i^1$ .<sup>13–15,17</sup>

This set of equations can be represented in a different way, employing the inverse of the unperturbed Hamiltonian operator  $(H_0 - \epsilon_i)^{-1}$ . In the case of a purely *local* perturbation potential, this formulation can be developed into an expression for the first order electronic density response  $n^{(1)}(\mathbf{r})$  as function of the perturbation potential,<sup>26</sup>

$$n^{(1)}(\mathbf{r}) = \int d\mathbf{r}' \chi(\mathbf{r}, \mathbf{r}') H_1(\mathbf{r}'). \quad (2)$$

In this formula,  $\chi(\mathbf{r}, \mathbf{r}')$  is the linear electronic susceptibility tensor, which allows the direct calculation of the perturbed electronic density without a self-consistent scheme. However, for the application of Eq. (2) the explicit shape of  $\chi(\mathbf{r}, \mathbf{r}')$  is required, a non-trivial computational task for a complex molecular system. In particular, the susceptibility tensor is a function of the inverse of the unperturbed Hamiltonian, which in principle requires the knowledge of the entire manifold of

<sup>a)</sup>Electronic mail: daniel.sebastiani@chemie.uni-halle.de

its eigenvalues and eigenstates (here, the Kohn-Sham energies and orbitals). To circumvent this problem, we make use of the Hermitian property of  $\chi(\mathbf{r}, \mathbf{r}')$ . This allows us to represent it by its eigenstates  $\chi_i(\mathbf{r})$  and eigenvalues  $\chi_i$ ,

$$\chi(\mathbf{r}, \mathbf{r}') = \sum_i \chi_i(\mathbf{r}) \chi_i \chi_i(\mathbf{r}'). \quad (3)$$

In a previous paper, we presented a computational scheme for the electronic susceptibility based on this representation and analysed the properties of the susceptibility eigenstates and eigenvalues in a water molecule. Furthermore, we benchmarked the scheme with response densities and the polarizability tensor. In the present work, we investigate how strongly the electronic susceptibility tensor depends on the molecular geometry of the underlying system. In this context, we also focus on the calculation of the electronic charge rearrangement due to geometric variations by means of the susceptibility determined at the equilibrium geometry. Specifically, we compute the electric dipole moment of a water molecule in different geometries by using the Coulomb potential difference between the geometries as perturbation potential in Eq. (2).

## II. COMPUTATIONAL SCHEME AND SYSTEM SETUP

### A. Calculation of the electronic susceptibility

Under the assumption that the eigenvalue spectrum of the electronic susceptibility features a fast decay, only a finite number of states contribute significantly to Eq. (3), and higher states have only a negligible contribution. This in turn would allow to truncate the summation after only a small part of the spectrum, using the largest eigenvalues only. This property of the linear electronic susceptibility tensor has been investigated in depth in a previous report.<sup>26</sup>

In our approach, the largest eigenvalues and eigenfunctions of the linear susceptibility tensor are computed using the iterative Lanczos diagonalization scheme. This scheme requires the application of the matrix that shall be diagonalized (i.e., the susceptibility tensor  $\hat{\chi}$ ) to an arbitrary vector. In the framework of DFT, the action of the electronic susceptibility tensor on a particular perturbation potential (yielding directly the first-order electronic response density) is realized in practice by solving the conventional perturbation theory equations for that specific potential<sup>13–15,17</sup> according to Eq. (1). The Lanczos diagonalization scheme for a matrix (here, the tensor  $\hat{\chi}$ ) consists now in repeatedly applying this tensor on the previous result (here, the response density). This protocol iteratively generates a series of functions/vectors, which form a growing so-called Krylov subspace. As the final step, the tensor is then projected into this subspace, and the resulting tridiagonal matrix is diagonalized. The quality of this diagonalization (i.e., the degree to which the eigenvalues/vectors in this subspace correspond to the values and vectors of the unprojected tensor) depends on the number of iterations performed, i.e., the dimension of the subspace.

### B. Dipole moments induced by geometrical changes

One possible application of the electronic susceptibility is the prediction of molecular dipole moments induced by geometrical distortions. When the molecular geometry is changed (from “geometry 1” to “geometry 2”), a change in the dipole moment is induced,

$$\mathbf{d}_{\text{induced}}^{\text{sc}} = \mathbf{d}_{\text{total}}^{\text{sc}}(\text{geo } 2) - \mathbf{d}_{\text{total}}^{\text{sc}}(\text{geo } 1), \quad (4)$$

where  $\mathbf{d}_{\text{total}}^{\text{sc}}$  are the dipole moments of the respective geometries. These are calculated directly from the ground-state charge density  $n_{\text{total}}(\mathbf{r})$ , which contains nuclear and electronic charges,

$$\mathbf{d}_{\text{total}}^{\text{sc}} = \int n_{\text{total}}(\mathbf{r}) \mathbf{r} d\mathbf{r}. \quad (5)$$

In common density functional theory, this requires two self-consistent wave function optimisations. Alternatively, the geometry variation can be seen as a perturbation, characterized by a perturbation Hamiltonian, which is just the difference of the nuclear Coulomb potential between the two geometries. This in turn enables the application of perturbation theory, either in its self-consistent formulation<sup>13–15,17</sup> or in the form presented above<sup>24–26,32</sup> using the linear electronic susceptibility tensor. In the framework of density functional theory using effective core potentials, the potential (see Eq. (6)) is composed from the nuclear electrostatic potential  $V_{\text{es}}$  and the local part of the effective core potential  $V_{\text{loc}}$ ,

$$V^{(1)}(\mathbf{r}) = V_{\text{es}}^{\text{geo } 2}(\mathbf{r}) - V_{\text{es}}^{\text{geo } 1}(\mathbf{r}) + V_{\text{loc}}^{\text{geo } 2}(\mathbf{r}) - V_{\text{loc}}^{\text{geo } 1}(\mathbf{r}). \quad (6)$$

The susceptibility approach requires the explicit knowledge of the tensor according to Eq. (3), but once its spectrum is computed in the equilibrium geometry, the electronic response to *any* molecular geometric change can be computed by means of relatively simple scalar products between the eigenstates and the perturbation potential. Hence, no explicit self-consistent calculation is needed to compute the correction to the charge density  $n_{\text{total}}^{(1)}(\mathbf{r})$  resulting from any geometric variation. The induced dipole moment  $\mathbf{d}_{\text{induced}}^{\chi}$  thus can be computed according to

$$\mathbf{d}_{\text{induced}}^{\chi} = \int n_{\text{total}}^{(1)}(\mathbf{r}) \mathbf{r} d\mathbf{r} \quad (7)$$

without any self-consistent electronic structure cycle other than the actual calculation of the spectrum of the electronic susceptibility. Eventually, the total dipole moment in the new geometry is then given by

$$\mathbf{d}_{\text{total}}^{\chi} = \mathbf{d}^{\text{sc}} + \mathbf{d}_{\text{induced}}^{\chi}. \quad (8)$$

### C. System setup

We chose the water molecule as a benchmark system for our approach, because of its enormous importance as solvent in physics, chemistry, and biology. Beyond the equilibrium geometry, we used several modified molecular structures which were chosen along the normal modes of the

water molecule (see Table I). These distorted structures are acquired by applying the linear approximation of the displacement caused by one vibrational mode with different prefactors to gain the desired energetic range. The actual atomic displacements from the equilibrium geometry were chosen such as to include deviations of different magnitude scales; the energetic differences relative to the equilibrium structure correspond to vibrational excitation temperatures of about 15 K, 375 K, 1200 K, and 3350 K of a single degree of freedom. In more chemical terms, they are approximately equal to 0.5%, 15%, 50%, and 150% of the strength of a hydrogen bond. All calculations were performed with the CPMD-package,<sup>33</sup> using a plane wave cutoff of 70 Ry. For the sake of simplicity, periodic boundary conditions were used in combination with a large supercell ( $12 \times 12 \times 12 \text{ \AA}$ ) to prevent interaction of a molecule with its periodic images. If not stated otherwise, Goedecker-Teter-Hutter pseudopotentials were used.<sup>34,35</sup>

We used the BLYP gradient-corrected exchange-correlation functional<sup>36,37</sup> which is commonly used in condensed-phase electronic structure calculations within periodic boundary conditions.<sup>27,38–40</sup> There is evidence that this functional gradually overestimates the strength of hydrogen bonds and the molecular polarizability.<sup>41–43</sup> However, the use of hybrid functionals including explicit orbital exchange operators yields a prohibitive computational cost in the framework of plane wave basis sets due to the nonlocality of the exchange operator in this basis. As a consequence, we use the BLYP functional also for our reference calculation. Nevertheless, it should be mentioned that the approach as such is not restricted to local and semi-local xc functionals, only our present implementation is.

Our basis set is composed of plane waves, which have no bias towards any molecular symmetries or atomic coordinates, and therefore has a very high dimensionality. Our plane wave cutoff corresponds to a total of 460 000 plane waves, which allow a great flexibility for the susceptibility eigenstates. This choice allows us to push the number of considered eigenvalues/eigenfunctions for the susceptibility up to a value of 7500. This number appears large, but has been chosen to investigate the dependence of the significance of the states as carefully as possible, and to ensure that we certainly reach proper basis set convergence for the spectrum of  $\chi$ .

### III. RESULTS

#### A. Eigenvalue spectrum convergence

To empirically validate the assumption of the fast decay of the eigenvalue spectrum, we have computed the relevant

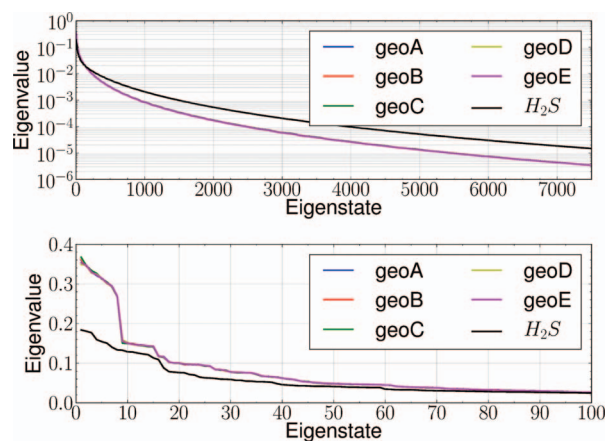


FIG. 1. Eigenvalue spectrum of the electronic susceptibility tensor  $\chi(\mathbf{r}, \mathbf{r}')$  of a water molecule in different geometries and a  $H_2S$  molecule in its ground state. The upper plot shows the 7500 largest eigenvalues on a logarithmic scale, the second one is a close-up version of the largest 100 states. In our calculations, we use atomic units, so that the response eigenvalues are obtained in elementary charges per hartree and cubic bohr.

fraction of the eigenvalue spectrum of a water and an  $H_2S$  molecule, shown in Figure 1. For both molecules, the shape of the spectrum exhibits the desired decay, with a somewhat slower decrease for  $H_2S$ . This effect is most likely due to the smaller HOMO/LUMO gap of the latter, resulting in the unoccupied molecular orbitals being accessible at lower excitation energies. When comparing the various geometries of the water molecule, we observe that the decay of the susceptibility spectrum of water is virtually invariant to geometric distortions.

#### B. Transferability

To judge the transferability of the eigenstates from one molecular geometry to another, we compare the individual eigenvalues and the spatial shape of corresponding eigenstates  $\chi_i(\mathbf{r})$  of our water molecule in two of the modified geometries (C and E, see Table I) with the equilibrium structure. The eigenvalue spectra for different  $H_2O$  geometries are shown in Figure 1. The eigenvalue spectrum shows no significant dependency on the geometry, even for the most significant eigenvalues (see the close-up at the bottom of Figure 1).

For the spatial shape of the eigenstates, it is sufficient to evaluate the absolute scalar product  $\int |\chi_i^{geo1}(\mathbf{r})\chi_i^{geo2}(\mathbf{r})|d\mathbf{r}$ . The absolute value is taken because Eqs. (2) and (3) are invariant under sign changes of  $\chi_i(\mathbf{r})$ . In Figure 2, the absolute scalar products between eigenstates obtained from three different geometries are shown. To take into account that the

TABLE I. Internal coordinates and energy differences (compared to geometry A, the equilibrium state) of the analysed water geometries.

$H_2O$	Excitation	$H_1 - O_1$ [pm]	$H_2 - O_1$ [pm]	$\angle H_1O_1H_2$ [deg]	$\Delta E_{geoA}$ [mHa]
Geometry A	Equilibrium	99.0	99.0	104.5	
Geometry B	Shear vibration	99.4	99.4	102.4	0.04
Geometry C	Shear vibration	100.9	100.9	96.3	1.19
Geometry D	Asymmetric stretch	91.3	107.3	104.6	10.63
Geometry E	Asymmetric stretch	94.2	103.9	104.6	3.82

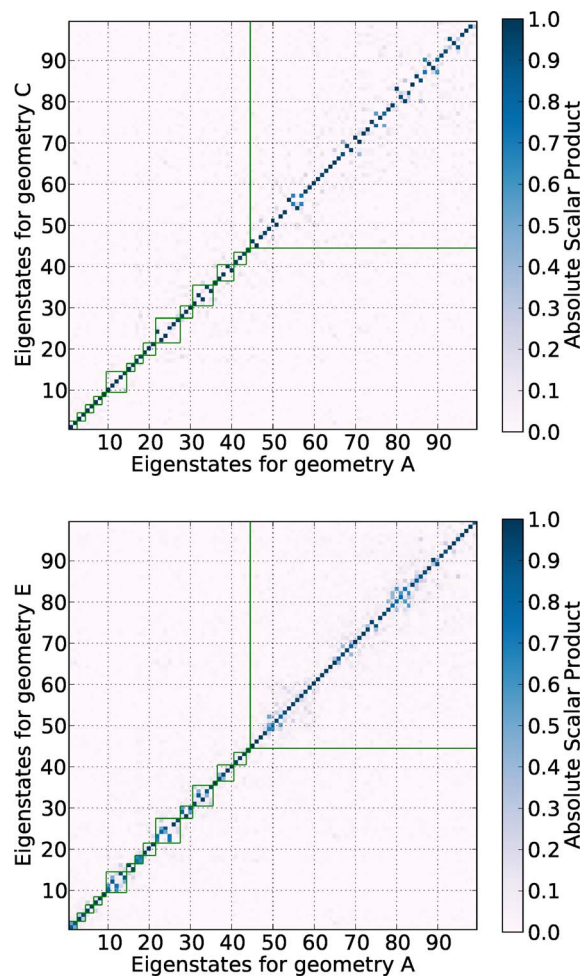


FIG. 2. Spatial overlap matrix of eigenstates from different  $H_2O$  geometries. The scalar product amplitudes are colour coded. The green boxes are manually chosen estimates for the spanned subspaces of degenerate states.

eigenstates are possibly degenerate, we estimated that eigenvalues which differ by less than 5% belong to the same subspace. This heuristic approach leads to the subspaces indicated by the green boxes in the plot. We compare the water equilibrium geometry (A) with two geometries obtained from vibrations, the shear vibration (C) and the asymmetric stretch (E) (see Table I). In both cases, all states originating from a given subspace in geometry A map into the corresponding subspace of geometry C/E. The main difference between the two cases is the degree of scattering of the minor overlap values around  $\approx 0.1$ . In the case of the shear vibration, the pattern is diffuse, while the asymmetric stretch shows a concentration close to main diagonal. We performed the same analysis to the susceptibilities computed with different pseudopotentials in the same molecular geometry (see the supplementary material<sup>44</sup>), resulting in no observable differences.

It should be noted that the degenerate subspaces of the eigenspectrum (visible as nonzero off-diagonal elements in the matrix of Figure 2) correspond to eigenfunctions which have approximately the same spatial shape but different symmetries. In the context of molecular orbitals, this would correspond to the symmetric and antisymmetric linear combinations of localized (non-canonical) orbitals. This is illustrated in the example of the eigenstate pair with numbers 22/24 of

the water molecule (see also the off-diagonal elements at positions 22 and 24 in Figure 2) in the supplementary material.<sup>44</sup>

### C. Dipole moments

An interesting follow-up question is whether it is possible to compute the structurally induced change in the molecular dipole moment by means of the electronic susceptibility. To investigate this, we computed the induced dipole moment  $\mathbf{d}_{\text{induced}}^X$  as well as the total dipole moment  $\mathbf{d}_{\text{total}}^X$  with the electronic susceptibility according to Eqs. (7) and (8). As a reference, we also calculated the total dipole moments  $\mathbf{d}_{\text{total}}^{\text{sc}}$  self-consistently (Eq. (5)), as well as the induced  $\mathbf{d}_{\text{induced}}^{\text{sc}}$  (Eq. (4)). Analysed are transitions from the equilibrium geometry to the geometries derived from vibrational excitations.

The final results of these calculations are listed in Table II and the convergence of the induced dipole moment is shown in Figure 3. The graphs indicate that the dipole moment converges quickly against its final value. A comparison of the values listed in the table shows that the susceptibility approach yields induced dipole moments of moderate accuracy with magnitude deviations below 16%, except for geometry C. The spatial orientation is reproduced correctly for geometries based on the shear vibration (B and C). However, the induced dipole is tilted up to  $26^\circ$  for the asymmetric stretch geometries. These deficiencies are most likely related to the perturbative character of our entire approach. It is important to note that after all, our susceptibility based calculation is only a *linear* correction of the molecular property (here, the dipole moments) to the perturbation (here, the geometric distortion). Quadratic or higher orders are not taken into account. Hence, from a purist point of view, the approach is only guaranteed to work for differentially small perturbations. Our actual perturbations are atomic displacements which correspond to a perturbing potential of the form  $V^{(1)}(\mathbf{r}) = Z/|\mathbf{r} - \mathbf{R}_{\text{new}}| - Z/|\mathbf{r} - \mathbf{R}_{\text{old}}|$ , and are thus by no means differentially small – in fact, they have as many poles as there are atoms in the molecule.

For the sake of completeness, we have performed two additional calculations of the induced dipole moment using a classical forcefield (flexible simple point charge (SPC)) and a high-level quantum chemical calculation (coupled cluster singles and doubles augmented by perturbative treatment of

TABLE II. Comparison between dipole moments obtained from self-consistent and electronic susceptibility calculations. Shown are the magnitudes of total and induced dipole moments, as well as the angle between  $\mathbf{d}^X$  and  $\mathbf{d}^{\text{sc}}$ . All susceptibility calculations started in the equilibrium geometry.

Property	Final geometry			
	GeoB	GeoC	GeoD	GeoE
$\ \mathbf{d}_{\text{induced}}^{\text{sc}}\ $ [D]	0.0295	0.114	0.196	0.118
$\ \mathbf{d}_{\text{induced}}^X\ $ [D]	0.0327	0.166	0.227	0.124
$\ \mathbf{d}_{\text{total}}^{\text{sc}}\ $ [D]	1.79	1.87	1.76	1.76
$\ \mathbf{d}_{\text{total}}^X\ $ [D]	1.79	1.92	1.86	1.79
$\langle\langle \mathbf{d}_{\text{total}}^X, \mathbf{d}_{\text{total}}^{\text{sc}} \rangle\rangle$ [deg]	0.00	0.00	0.16	0.04
$\langle\langle \mathbf{d}_{\text{induced}}^X, \mathbf{d}_{\text{induced}}^{\text{sc}} \rangle\rangle$ [deg]	0.05	0.01	25.96	17.07

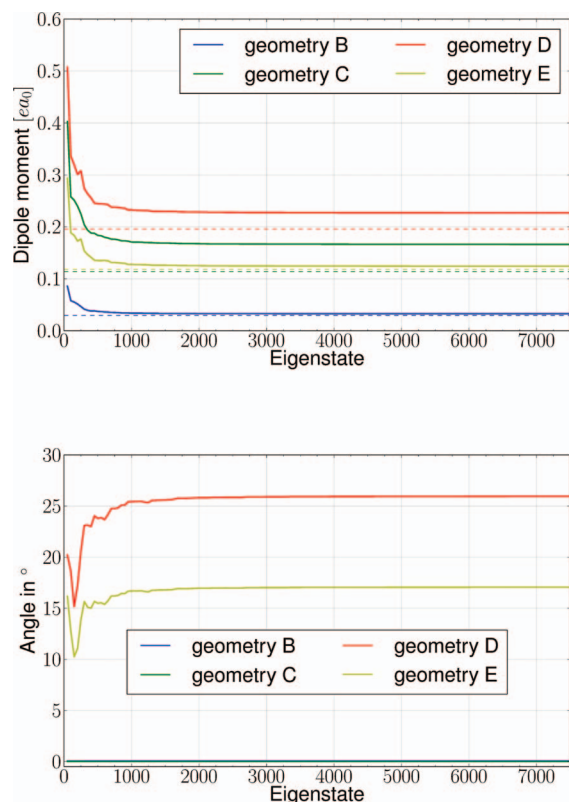


FIG. 3. Convergence of the induced dipole moments. The upper figure shows the magnitude of the induced dipole moments as function of the number of eigenstates incorporated, along with the corresponding target value from the self-consistent calculation (cf. Table II). The lower plot shows the angle between the induced dipole moment calculated with the electronic susceptibility and the self-consistent reference.

triples (CCSD(T)) with aug-cc-pvtz). The results from these calculations are listed in Table III. As expected, the *ab initio* dipole moment and the distortion-induced polarization of the self-consistent DFT and the perturbative DFT calculations are very close. The *ab initio* reference calculation at the CCSD(T) level is about 5% (dipole moment) and 10% (polarization) larger, whereas the force field based values are off by 30% (dipole moment) and 100% (polarization). This indicates that there is a promising perspective for a perturbation theory based calculation of electrostatic properties of strongly polar (and polarizable) systems. It should be noted that it is in principle straightforward to compute the linear susceptibility tensor within our scheme on the basis of any other level of electronic structure theory (be it DFT/B<sub>3</sub>LYP or coupled-cluster theories), which would again increase the predictive power and numerical reliability.

TABLE III. Comparison of dipole moments from different levels of theory for geometry C. The spatial orientation of the dipole is the same in all cases (not shown).

Property	Computational method			
	DFT/sc	DFT/ $\chi$	CCSD(T)	SPC-forcefield
$\ \mathbf{d}_{\text{total}}\ $ [D]	1.87	1.92	2.00	2.59
$\ \mathbf{d}_{\text{induced}}\ $ [D]	0.114	0.116	0.126	0.256

## IV. CONCLUSION

In this work, we have shown that the linear electronic susceptibility tensor of a molecule can be used to compute the electronic charge displacement due to a variation in molecular geometry. Our calculations show that the electronic susceptibility has virtually no dependency on the geometry up to conformational energies of 10 mHa. Therefore, it is in principle possible to describe the electronic density distribution of a molecule (here, the water molecule) in an arbitrary geometry at high accuracy, using exclusively the (fixed) charge distribution and the linear response tensor in the equilibrium geometry.

Our computational scheme is able to reproduce the electric dipole of a fully self-consistent calculation in several geometries which are several  $k_B T$  (at room temperature) above the equilibrium geometry. The calculations of the dipole moment of a water molecule yield accurate total dipole moments with minor magnitude deviations and correct spatial orientation. The induced dipole moments are less accurate, having moderate magnitude errors. In the case of the symmetry breaking asymmetric stretch vibration, the orientation of the induced dipole moment is somewhat tilted with respect to the reference calculation. It should be noted that an obvious subsequent step, the calculation of atomic forces and the Hessian matrix by means of our approach, is *in principle* a straightforward extension. However, in practice, we encountered the difficulty that the nonlocal projectors in our effective core potentials significantly contribute to the Hessian matrix, while the susceptibility approach is by design not able to take these contributions into account.

These results show that the non-self-consistent approach of computing electronic density variations by means of the explicit susceptibility tensor opens the path towards a molecular dynamics scheme with DFT accuracy and full atomic flexibility at a fraction of the computational cost of a self-consistent calculation. A future perspective for the improvement of the results is the representation of the response functions via an atom-centered Gaussian basis set. In such a basis set, the dipole moment calculation can be performed analytically instead of numerically by integration on a real-space grid.

<sup>1</sup>N. B. Colthup, L. H. Daly, and S. E. Wiberley, *Introduction to Infrared and Raman Spectroscopy* (Academic Press, New York, 1975).

<sup>2</sup>B. E. Warren, *X-Ray Diffraction* (Dover, Mineola, 1990).

<sup>3</sup>D. Porezag and M. R. Pederson, *Phys. Rev. B* **54**, 7830 (1996).

<sup>4</sup>J. Van Kranendonk and M. Walker, *Phys. Rev. Lett.* **18**, 701 (1967).

<sup>5</sup>J. F. Moulder, W. F. Stickle, P. E. Sobol, and K. D. Bomben, *Handbook of X Ray Photoelectron Spectroscopy* (Perkin-Elmer Corporation (Physical Electronics), 1992).

<sup>6</sup>A. Dreuw, *ChemPhysChem* **7**, 2259 (2006).

<sup>7</sup>M. Wanko, M. Hoffmann, P. Strodet, A. Koslowski, W. Thiel, F. Neese, T. Frauenheim, and M. Elstner, *J. Phys. Chem. B* **109**, 3606 (2005).

<sup>8</sup>B. Kirchner, F. Wennmohs, S. Ye, and F. Neese, *Curr. Opin. Chem. Biol.* **11**, 134 (2007).

<sup>9</sup>W. Thiel, *Chimia* **58**, 276 (2004).

<sup>10</sup>W. Thiel, *Angew. Chem., Int. Ed. Engl.* **50**, 9216 (2011).

<sup>11</sup>C. Frischkorn and M. Wolf, *Chem. Rev.* **106**, 4207 (2006).

<sup>12</sup>M. Quack, *Annu. Rev. Phys. Chem.* **41**, 839 (1990).

<sup>13</sup>X. Gonze, *Phys. Rev. A* **52**, 1086 (1995).

<sup>14</sup>X. Gonze, *Phys. Rev. A* **52**, 1096 (1995).

<sup>15</sup>S. Baroni, S. De Gironcoli, A. Del Corso, and P. Giannozzi, *Rev. Mod. Phys.* **73**, 515 (2001).

<sup>16</sup>D. Rocca, D. Lu, and G. Galli, *J. Chem. Phys.* **133**, 164109 (2010).

- <sup>17</sup>A. Putrino, D. Sebastiani, and M. Parrinello, *J. Chem. Phys.* **113**, 7102 (2000).
- <sup>18</sup>D. B. Chesnut, *Chem. Phys. Lett.* **246**, 235 (1995).
- <sup>19</sup>D. Sebastiani and U. Röthlisberger, *J. Phys. Chem. B* **108**, 2807 (2004).
- <sup>20</sup>J. Vaara, *Phys. Chem. Chem. Phys.* **9**, 5399 (2007).
- <sup>21</sup>M. P. Ljungberg, A. P. Lyubartsev, A. Nilsson, and L. G. M. Pettersson, *J. Chem. Phys.* **131**, 034501 (2009).
- <sup>22</sup>H. M. Petrilli, P. E. Blochl, P. Blaha, and K. Schwarz, *Phys. Rev. B* **57**, 14690 (1998).
- <sup>23</sup>D. Benoit, D. Sebastiani, and M. Parrinello, *Phys. Rev. Lett.* **87**, 226401 (2001).
- <sup>24</sup>H. F. Wilson, F. Gygi, and G. Galli, *Phys. Rev. B* **78**, 113303 (2008).
- <sup>25</sup>H. F. Wilson, D. Lu, F. Gygi, and G. Galli, *Phys. Rev. B* **79**, 245106 (2009).
- <sup>26</sup>A. Scherrer, V. Verschinin, and D. Sebastiani, *J. Chem. Theory Comput.* **8**, 106 (2012).
- <sup>27</sup>R. O. Jones and O. Gunnarsson, *Rev. Mod. Phys.* **61**, 689 (1989).
- <sup>28</sup>D. Marx and J. Hutter, *Ab Initio Molecular Dynamics: Basic Theory and Advanced Methods* (Cambridge University Press, Cambridge, 2009), p. 578.
- <sup>29</sup>S. Piscanec, M. Lazzeri, J. Robertson, A. C. Ferrari, and F. Mauri, *Phys. Rev. B* **75**, 035427 (2007).
- <sup>30</sup>F. Rossi, *Rev. Mod. Phys.* **74**, 895 (2002).
- <sup>31</sup>A. H. C. Neto, F. Guinea, N. M. R. Peres, K. S. Novoselov, and A. K. Geim, *Rev. Mod. Phys.* **81**, 109 (2009).
- <sup>32</sup>D. Lu, F. Gygi, and G. Galli, *Phys. Rev. Lett.* **100**, 147601 (2008).
- <sup>33</sup>J. Hutter, D. Marx, P. Focher, M. Tuckerman, W. Andreoni, A. Curi-  
oni, E. Fois, U. Rothlisberger, P. Giannozzi, T. Deutsch, A. Alavi, D.  
Sebastiani, A. Laio, J. VandeVondele, A. Seitsonen, S. Billeter, and M.  
Parrinello, *Computer Code CPMD, version 3.12* (IBM Corp. and MPI-FKF  
Stuttgart, 2007).
- <sup>34</sup>S. Goedecker, M. Teter, and J. Hutter, *Phys. Rev. B* **54**, 1703 (1996).
- <sup>35</sup>C. Hartwigsen, S. Goedecker, and J. Hutter, *Phys. Rev. B* **58**, 3641 (1998).
- <sup>36</sup>A. D. Becke, *Phys. Rev. A* **38**, 3098 (1988).
- <sup>37</sup>C. Lee, W. Yang, and R. G. Parr, *Phys. Rev. B* **37**, 785 (1988).
- <sup>38</sup>P. Carloni, U. Röthlisberger, and M. Parrinello, *Acc. Chem. Res.* **35**, 455 (2002).
- <sup>39</sup>B. Kirchner, *Phys. Rep., Phys. Lett.* **440**, 1 (2007).
- <sup>40</sup>C. Schiffrmann and D. Sebastiani, *Phys. Status Solidi B* **249**, 368 (2012).
- <sup>41</sup>B. Auer, R. Kumar, J. R. Schmidt, and J. L. Skinner, *Proc. Natl. Acad. Sci. U.S.A.* **104**, 14215 (2007).
- <sup>42</sup>D. R. Banyai, T. Murakhtina, and D. Sebastiani, *Magn. Reson. Chem.* **48**, S56 (2010).
- <sup>43</sup>B. Santra, A. Michaelides, M. Fuchs, A. Tkatchenko, C. Filippi, and M. Scheffler, *J. Chem. Phys.* **129**, 194111 (2008).
- <sup>44</sup>See supplementary material at <http://dx.doi.org/10.1063/1.4819070> for additional data about the dependence of the susceptibility eigenstates on the choice of the pseudopotential, as well as an illustration of the shape of eigenstates from a degenerate subspace.